



Published in final edited form as:

Traffic. 2002 February ; 3(2): 124–132.

Melanophilin, the Product of the *Leaden* Locus, is Required for Targeting of Myosin-Va to Melanosomes

D. William Provance Jr, Ted L. James, and John A. Mercer*

McLaughlin Research Institute, 1520 23rd St South, Great Falls, MT 59405, USA

Abstract

The formation of complex subcellular organelles requires the coordinated targeting of multiple components. Melanosome biogenesis in mouse melanocytes is an excellent model system for studying the coordinated function of multiple gene products in intracellular trafficking. To begin to order events in melanosome biogenesis and distribution, we employed the classical coat-color mutants *ashen*, *dilute*, and *leaden*, which affect melanosome distribution, but not melanin synthesis. The loci have been renamed *Rab27a*, *Myo5a*, and *Mlph* for their gene products. While each of the three loci has been shown to be required for melanosome distribution, the point(s) at which each acts is unknown. We have utilized primary melanocytes to examine the interdependencies between *rab27a*, myosin-Va, and melanophilin. The localization of *rab27a* to melanosomes did not require the function of either myosin-Va or melanophilin, but *leaden* function was required for the association of myosin-Va with melanosomes. In *leaden* melanocytes permeabilized before fixation, myosin-Va immunoreactivity was greatly attenuated, suggesting that myosin-Va is free in the cytoplasm. Finally, we have complemented both the *leaden* and *ashen* phenotypes by cell fusion and observed redistribution of mature melanosomes in the absence of both protein and melanin synthesis. Together, our data suggest a model for the initial assembly of the machinery required for melanosome distribution.

Keywords

ashen; *dilute*; *leaden*; melanophilin; melanosomes; myosin-Va; *rab27a*; TRP-1

A central goal of cell biology is the identification and understanding of the molecular mechanisms that underlie the identity, assembly, and transport of organelles. In mammalian melanocytes, the formation of the melanosome is thought to occur through the convergence of multiple pathways for the delivery of the enzymes required for melanin synthesis. Trafficking of these enzymes involves the endoplasmic reticulum, trans-Golgi network, clathrin- and nonclathrin-coated vesicles, and endosomes (1–7).

Loci other than those that encode melanogenic enzymes also influence the coat colors of mice (8). Mutations at many of these loci affect other systems, including the nervous system and immune system. A subset of coat-color mutants (*dilute*, *ashen* and *leaden*) has been identified that synthesize normal levels of melanin, but inefficiently transfer melanosomes to neighboring cells (9–11). This leads to a clumping of melanin granules in the hair shaft, decreasing the amount of light absorbed. All three loci have been cloned and renamed *Myo5a*, *Rab27a*, and *Mlph*, respectively (12–14). The *Myo5a* (*dilute*) locus encodes myosin-Va (12), a processive molecular motor (15–17). Mutations in the human *MYO5A* gene underlie some cases of Griscelli Syndrome (18). Rab proteins, members of the ras superfamily of small GTPases, are

* Corresponding author: John A. Mercer, umbjm@montana.edu.

involved in multiple pathways of vesicle trafficking (19,20). Mutations in *Rab27a* cause the *ashen* phenotype in mice (13) and a subset of Griscelli syndrome cases in humans (21,22).

In culture, wild-type primary melanocytes have a uniform distribution of melanosomes throughout the cytoplasm. Melanosomes from *Myo5a^d*, *Rab27a^{ash}*, or *leaden* homozygous mutant mice, however, accumulate around the nucleus (13,23,24). Genetic analysis of compound mutants between the *Myo5a^d*, *Rab27a^{ash}*, and *leaden* loci showed little synergy in affecting coat color phenotype (25), suggesting that they may act within the same pathway. Furthermore, the dilution of coat color caused by all three mutations is suppressed by a mutation at a fourth locus, *dilute suppressor* (25).

While the evidence that all three genes are required for melanosome distribution is unequivocal, the evidence that they are components of the actual machinery mediating distribution is circumstantial at best. Initial examinations of mutant melanosomes have suggested that melanosome biogenesis is normal (10,24). Therefore, it has been hypothesized that a complex consisting of myosin-Va, rab27a, and melanophilin is formed and targeted to the melanosome, during or after its genesis, to allow its distribution (26). Others have previously shown (27, 28) that Rab27a is required for the interactions between myosin-Va and melanosomes. In this study, we show that *leaden* function also is required for the interaction of myosin-Va with melanosomes. Others have shown that *Rab27a^{ash}* mutant phenotype can be rescued by transfection (28), but we show that mature melanosomes assembled in the absence of either Rab27a or melanophilin can be redistributed by fusion of mutant with wild-type cells or of the two mutants with each other, even during inhibition of melanin and protein synthesis.

Results

Myosin-Va distribution is altered in *leaden* melanocytes

If myosin-Va and melanophilin act independently in the targeting of myosin-Va to melanosomes, then we predict that myosin-Va would be associated with melanosomes in *leaden* mutant melanocytes. Conversely, if delivery of myosin-Va to melanosomes depends on *leaden* function, either to form a complex prior to or coincident with melanosome association, then myosin-Va would be expected to display an altered distribution in *leaden* mutant melanocytes. Our data (Figure 1) support the latter hypothesis.

The distribution of myosin-Va in wild-type melanocytes is shown in Figure 1(A,E,I). Because the bright-field image is not confocal, we used TRP-1 as a melanosomal marker to assess colocalization of myosin-Va with melanosomes in panels I, J, K, and L. As observed previously, myosin-Va had a punctate pattern throughout the cytoplasm and showed colocalization with melanosomes in the representative wild-type melanocyte (Figure 1I). Next, the distribution of myosin-Va was assessed in *leaden* melanocytes and compared to melanosomes. As expected, the bright-field images showed a perinuclear accumulation of melanosomes (Figure 1F). In a representative *leaden* melanocyte, myosin-Va had a more diffuse signal in the melanosome-free cytoplasm with a pronounced decrease in fluorescence in the perinuclear region. The merged image further demonstrates that much of the myosin-Va signal was not associated with melanosomes (Figure 1J). Myosin-Va was not detected in *Myo5a* (*dilute*) melanocytes (Figure 1C,K), demonstrating the specificity of our antibody (29).

As an additional control, we found that myosin-Va also was dramatically mislocalized in *Rab27a^{ash}/Rab27a^{ash}* melanocytes (Figure 1D,H,L), as it was more diffuse in the periphery and the weaker perinuclear signal was concentrated to one side of the nucleus. In comparison, the wild-type cell had a punctate myosin-Va fluorescent localization that was evenly distributed (compare Figure 1A to Figure 1D). These data are consistent with those first published by Hume et al. (27), and later by Wu et al. (28).

The more diffuse distribution of myosin-Va in *leaden* melanocytes suggested that a large proportion of myosin-Va was free in the cytoplasm. To test this hypothesis, we permeabilized wild-type, *leaden*, and *Rab27a^{ash}/Rab27a^{ash}* melanocytes with Triton X-100 before fixation with methanol and acetone. Control melanocytes were fixed before permeabilization, and myosin-Va was detected by confocal immunofluorescent microscopy. Fluorescence per unit area was calculated and the data are presented in Figure 2. There was no significant reduction in fluorescence in wild-type melanocytes, but fluorescence in both *leaden* and *Rab27a^{ash}/Rab27a^{ash}* melanocytes was significantly reduced, consistent with most of the myosin-Va being free (or in small, freely diffusible complexes) in the mutant cells, rather than stably interacting with melanosomes and other organelles.

Rab27a distribution is partially coincident with melanosomes in *leaden* mutant melanocytes

To establish a temporal sequence for the function of these three genes, we next examined the intracellular distribution of rab27a in our panel of primary melanocytes (Figure 3). In wild-type melanocytes, the punctate fluorescent signal that represents Rab27a distribution partially coincided with the location of pigmented melanosomes (Figure 3A,E). Regions that showed few or no mature melanosomes by bright-field microscopy had a corresponding decrease in rab27a reactivity. In *leaden* (Figure 3B,F) and *Myo5a (dilute)* (Figure 3C,G) mutant melanocytes, the distribution of rab27a again closely correlated with mature melanosomes, which accumulate around the nucleus. Therefore, the obvious changes seen for myosin-Va distribution in *leaden* and *Rab27a^{ash}/Ra-b27a^{ash}* melanocytes were not observed for the distribution of rab27a in *leaden* and *dilute* mutant melanocytes.

The mouse monoclonal antibody utilized to detect rab27 gave two distinct patterns in wild-type, *leaden*, and *Myo5a (dilute)* melanocytes: punctate and fibrous. To determine which part of the staining pattern was a representation of rab27a localization, the monoclonal antibody against rab27 was used to stain *Rab27a^{ash}/Rab27a^{ash}* melanocytes, a genetic control for rab27a reactivity. Only the fibrous pattern was observed in the mutant melanocytes, indicating that the punctate pattern in cells of other genotypes represents rab27a distribution, while the fibrous pattern represents background or a cross-reacting antigen(s). Background was further reduced by adsorption with acetone powder made from the spleen of a *Rab27a^{ash}/Rab27a^{ash}* mouse (data not shown).

Two other factors complicate interpretation of the data for rab27a distribution; both lead to an underestimate of colocalization. First, the transmitted-light micrographs have a greater depth of field than the confocal micrographs. Second, the perinuclear accumulation of melanosomes potentially attenuates fluorescence in all three mutant melanocytes. However, despite these complications, these data suggest that the interaction of rab27a with melanosomes is not dependent on either melanophilin or myosin-Va.

The accumulation of mature melanosomes caused by the absence of melanophilin function can be rescued by fusion with wild-type cells

The lack of melanosomal myosin-Va localization in *leaden* mutant melanocytes suggests that the *leaden* gene product, melanophilin, may function early in melanosome biogenesis, maturation, or distribution. To test this hypothesis, we determined if mature melanosomes formed in *leaden* mutant melanocytes could be uniformly distributed upon introduction of melanophilin by cell–cell fusion.

Albino melan-c cells were fused to *leaden* mutant melanocytes with polyethylene glycol. Since no antibodies against melanophilin were available, we could not identify heterotypic fusion events using melanophilin as a marker. Therefore, we used CellTracker™ (Molecular Probes) to label the melan-c cells, and identified fusion events on the basis of fluorescence and

pigmented melanosomes. Cells that were identified as products of heterotypic fusion events had mature melanosomes that were dispersed throughout the cytoplasm (Figure 4, arrows). Pigmented melanocytes that did not contain CellTracker™ and therefore were not fused to melan-c cells maintained a perinuclear concentration of melanosomes (Figure 4, filled arrowheads).

After fusion, samples were split four ways and cultured in medium alone (data not shown); with phenylthiourea (PTU, a tyrosinase inhibitor that prevents pigmentation) (30,31); with cycloheximide (CH), to inhibit protein synthesis and thereby limit melanophilin available for rescue to the pool(s) already present in the melan-c cytoplasm at the time of fusion; or with both PTU and CH. Cells fused and treated with PTU had dispersed and dendritic melanosomes (Figure 4A, arrow), while a nonfused *leaden* melanocyte (Figure 4A, filled arrowhead) maintained its perinuclear melanosome distribution.

CH treatment did not prevent melanosome dispersion in fused cells (Figure 4B), although these cells had a more arborized morphology. The *leaden* mutant melanocytes that were not fused to melan-c cells maintained the *leaden* phenotype in cycloheximide (Figure 4B, filled arrowhead). The efficacy of inhibition of protein synthesis by CH in this protocol was greater than 90% as assessed by autoradiography in the presence of ³⁵S-methionine (the cells divide too infrequently to allow more conventional assessments). CH-treated cells produced 150 ± 39 silver grains, while untreated cells produced 1743 ± 440 silver grains. The PTU concentration used (200 μM) is twice the concentration that gives nearly complete inhibition of tyrosinase in B16 melanoma cells (32); in proliferating primary melanocytes, 200 μM PTU treatment reduces numbers of visible melanosomes 4-fold after 5 days (data not shown).

Even in the presence of both PTU and CH, pigmented melanosomes in fused cells were distributed normally (Figure 4C). Therefore, the rescue does not appear to be dependent on protein synthesis or new melanosome biogenesis. As a negative control, melan-c cells mixed with *leaden* melanocytes were plated in the absence of PEG and cultured in the presence of PTU and CH (Figure 4D). All pigmented cells in the controls had a perinuclear accumulation of melanosomes.

The accumulation of mature melanosomes caused by the absence of *rab27a* function can be rescued by fusion with wild-type cells

The altered myosin-Va distribution in *Rab27a* mutant melanocytes (27,28) (Figure 1D,H,L) indicates an early function for *rab27a* as well. We therefore performed a cell fusion experiment analogous to that shown in Figure 4 with *Rab27a^{ash}/Rab27a^{ash}* mutant melanocytes. Heterotypic fusion events were identified by both *rab27a* immunofluorescence (data not shown) and pigmented melanosome distribution (Figure 5). In these cases of heterotypic fusion, *Rab27a^{ash}/Ra-b27a^{ash}* melanocytes (*Tyr⁺/Tyr⁺*) contribute the pigmented melanosomes and melan-c cells (*Tyr^c/Tyr^c*, *Rab27a⁺/Rab27a⁺*) contribute *rab27a*.

The results were similar to those obtained with *leaden* melanocytes. After fusion, samples were split 4 ways as described above. As in panel 3 A, *Rab27a^{ash}/Rab27a^{ash}* mutant melanocytes that were not fused to melan-c cells maintained their melanosome distribution phenotype in CH (Figure 5B, filled arrowheads). In the presence of both PTU and CH, pigmented melanosomes in fused cells were distributed normally (Figure 5C). As described above, a mock fusion was performed by mixing melan-c cells with *Rab27a^{ash}/Ra-b27a^{ash}* melanocytes in the absence of PEG and culturing in the presence of PTU and CH (Figure 5D). All pigmented cells in the negative controls had a perinuclear accumulation of melanosomes.

Reciprocal complementation in fusions between *leaden* and *Rab27a^{ash}/Rab27a^{ash}* mutant melanocytes

The successful rescue of both *leaden* and *ashen* phenotypes by fusion with wild-type cells suggested that the mutants would rescue each other. Therefore, we tested for reciprocal complementation by fusing *leaden* with *ashen* (*Rab27a^{ash}/Rab27a^{ash}*) mutant melanocytes in the same manner. Restoration of melanosome distribution was observed in untreated cells (Figure 6A) as well as cells treated with both PTU and CH (Figure 6B). Rescue was observed in cells treated with either inhibitor alone as well (data not shown). No restoration was observed in control homotypic fusions or heterotypic mixtures in the absence of PEG (data not shown).

Discussion

While significant progress in understanding the delivery of melanogenic enzymes to melanosomes has been made (1–7), the identification of components functioning in the motility, distribution, and transfer of melanosomes to other cells is important as well (33,34) and has been relatively neglected until a spate of studies published in the last 6 years. The *Rab27a^{ash}*, *Myo5a^d*, and *leaden* mutants are ideal for studying distribution, since the levels of melanin in mutant mice are not different from wild-type levels; only melanosome distribution is abnormal and accounts for the dilution of coat color (8,10,13,24,35). The apparent maturity of melanosomes in these mutants suggests separate pathways for the acquisition of melanogenic and motile components by melanosomes (8,10,24). Using these mutants and others, we should be able to derive the temporal sequence of events required for melanosome assembly and distribution. Melanophilin, *rab27a*, and myosin-Va have been hypothesized to function in a complex that mediates the movement or capture of mature melanosomes (13, 14). We tested this model using *Rab27a^{ash}*, *Myo5a^d*, and *leaden* (now *Mlph*) homozygous mutant melanocytes. In all cases, our results do not exclude the possibility that *rab27a*, myosin-Va, and/or melanophilin are targeted to (and function to localize) a precursor organelle that subsequently fuses with melanosomes, providing them with other components of the motility machinery.

If independent pathways deliver melanophilin, *rab27a*, and myosin-Va, delivery of *rab27a* to melanosomes should not be dependent on myosin-Va function. This prediction was confirmed by the melanosomal localization of *rab27a* in *dilute* (*Myo5a^d/Myo5a^d*) mutant melanocytes (Figure 3C,G). In addition, *rab27a* partially colocalized with melanosomes in *leaden* mutant melanocytes, indicating that it is not necessary for *rab27a* to interact with either myosin-Va or melanophilin for its targeting to melanosomes (Figure 3B,F). The reciprocal experiments, however, suggested dependency, since both melanophilin and *rab27a* were required for myosin-Va binding to melanosomes. Two other groups (27,28) have previously published the latter observation.

Our observation that myosin-Va targeting requires melanophilin suggested that assembly of any motility/capturing complex on melanosomes might require melanophilin early in melanosome biogenesis. The result of our cell fusion experiment was not consistent with this hypothesis, since the introduction of melanophilin to melanosomes that were formed in its absence resulted in a uniform distribution of mature melanosomes (Figure 4); the same result was obtained for *Rab27a^{ash}/Rab27a^{ash}* mutants rescued by fusion with melan-c melanocytes (Figure 5), and the mutant melanocytes fused with each other (Figure 6). These data indicate that neither melanophilin nor *rab27a* function is required until after all the components necessary for pigmentation have been delivered and are functional. It further suggests that melanosomes have a mechanism for melanophilin and *rab27a* delivery that diverges from that of lysosomes. This is an important consideration since the melanosome has been widely considered to be a derivative of the lysosome (36–39), but recent data suggest significant differences (7). The results presented here appear to conflict with our previously published

immunofluorescence results (24); however, those experiments were performed with an antibody against a peptide. The antibody used in this study has been tested more extensively, and is more specific in both Western blotting and immunofluorescence (29) (data not shown). Also, the earlier experiments were performed using only methanol fixation, which may have allowed the differential loss of myosin-Va immunoreactivity during subsequent steps, given the data presented in Figure 2.

Melanophilin was recently identified as the product of the *leaden* gene (14) and is related to Slp3-a (40), the granophilins (41), and rabphilin (42). These sequence similarities suggest that melanophilin functions in the same manner as rabphilin (14), the best-characterized member of the family, and the data presented here strongly support that hypothesis, consistent with *rab27a* and melanophilin as 'co-keystones' for the assembly of distribution components. Our cell fusion experiments suggest that this assembly occurs independently of, and possibly after, the delivery of components involved in melanogenesis. It must be emphasized that our experiments cannot directly address the existence of any hypothesized motility complex consisting of myosin-Va, *rab27a*, and melanophilin. However, they do suggest that if such a complex exists, *rab27a* and melanophilin, either simultaneously or sequentially, provide a foundation for the interaction of myosin-Va with melanosomes. The recent cloning of the *leaden* gene (14) should allow the further dissection of these pathways.

Materials and Methods

Mice

Myo5a mutant mice (C57BL/6 J *Myo5a^d/Myo5a^d* and C57BL/6 J *Myo5a^{d-l}/Myo5a^d*) were a gift from Nancy Jenkins and Neal Copeland (National Cancer Institute-Frederick Cancer Research and Development Center). Mutant *Rab27a^{ash}* (C3H/HeSN-*ash/ash*) and *leaden* (C57BL/6 J *b/b ln/ln*) mice were purchased from the Jackson Laboratory (Bar Harbor, ME).

Tissue culture

Primary melanocytes were isolated from 1- to 3-day-old pups as previously described (24) and cultured in MGM-2 (Clonetics, San Diego, CA, USA) supplemented with 10 ng/ml recombinant mouse stem cell factor (Sigma, St. Louis, MO, USA). Melan-c cells were kindly provided by Dorothy Bennett and maintained in RPMI, 10% fetal bovine serum, 55 μ M β -mercaptoethanol, and 200 nM phorbol 12-myristate 13-acetate. Cells were plated onto 22-mm² coverslips 24–48 h prior to performing immunofluorescence.

Immunofluorescence

Primary melanocytes or melan-c cells grown on glass coverslips were rinsed in PBS and fixed for 5 min in -20°C methanol, followed by 30 s in -20°C acetone. Fixed cells were rehydrated in PBS for 5 min followed by two 5-min incubations in PBS with 10 mg/ml BSA. For exposure to primary antibody, cells were incubated for 1 h at room temperature with antibodies against *rab27* (mouse monoclonal diluted 1 : 100, BD Transduction Laboratories, San Diego, CA, USA) or antibodies against myosin-Va [mouse poly-clonal serum diluted 1 : 500 (29)] and TRP-1 [rabbit polyclonal serum diluted 1 : 750, gift from Vincent Hearing, NIH (43)]. Primary antibodies were diluted in PBS with 10 mg/ml BSA and 10% normal goat serum (Sigma). Cells were then rinsed 3 times for 5 min in PBS with 10 mg/ml BSA before simultaneous exposure to Alexa 488-labeled goat anti-mouse IgG (1 : 3000 dilution, Molecular Probes, Eugene, OR, USA) and Alexa 546-labeled goat anti-rabbit IgG (1 : 3000 dilution, Molecular Probes) for 30 min at room temperature. Finally, cells were rinsed 3 times for 5 min in PBS and mounted in AquaPolymount (Polysciences, Inc, Warrington, PA, USA). For the experiments in which melanocytes were permeabilized before fixation, coverslips were incubated in PBS containing

0.1% Triton X-100 for 10 min, quickly rinsed in PBS and fixed in methanol and acetone as described above.

Cell fusion

Melan-c cells (1×10^4), *Rab27a^{ash}* melanocytes, or *leaden* melanocytes (1×10^4) were combined pairwise in centrifuge tubes and pelleted. Prior to fusion with *leaden* melanocytes, melan-c cells were loaded with 10 μ M CellTracker™ (Molecular Probes) for 1 h, washed 3 \times , and cultured for 3 h in medium before trypsinization. Cells were gently resuspended in 25 μ l of RPMI with 10 ng/ml phytohemagglutinin and incubated 2 min at 37 °C. Next, 25 μ l of 50% polyethylene glycol/10% DMSO was added, mixed by flicking the tube, and incubated at 37 ° for 1 min. Then, 500 μ l of RPMI was added, mixed by flicking, and the cells were pelleted. The supernatant was removed, cells were resuspended in 400 μ l MGM-2, and plated onto four 18-mm² coverslips. Cells were allowed to attach to the coverslip for 45 min and then incubated 24 h in MGM-2 alone, MGM-2 with 200 μ M phenylthiocarbamide (phenylthiourea, PTU), MGM-2 with 1 μ g/ml cycloheximide (CH), or MGM-2 with 200 μ M PTU and 1 μ g/ml CH. Cells were then processed for immunofluorescence as described above. Inhibition of protein synthesis by CH was assayed by autoradiography of melan-c cells treated with cycloheximide as described above in the presence of 50 μ Ci/ml ³⁵S-methionine (EasyTag™, New England Nuclear, Boston, MA). Coverslips were attached to slides, dipped in Kodak NTB-2 emulsion and exposed for 2 days at 4 °C.

Microscopy

All images were obtained on a Nikon Optiphot-2 equipped with either a 60 \times PlanApo lens (NA 1.4, Nikon) or 20 \times Fluor lens (NA 0.75, Nikon) and a MicroRadiance confocal scanning system (Bio-Rad, Hercules, CA, USA). Images were collected with Kalman averaging by LaserSharp software (Version 3.2, Bio-Rad) and processed within Adobe Photoshop.

Acknowledgements

We thank George Carlson, John Bermingham, Dennis Stephenson, Corike Nuike, and Colleen Silan for reviewing the manuscript, and George Lang-ford for suggesting the permeabilization experiment. This work was supported by NSF grant 9874907. D.W.P. was supported by a grant from the Oberkotter Foundation. T.L.J. participated in the Summer Intern Program at the McLaughlin Research Institute and was supported by the Montana Chapter of the American Cancer Society.

References

1. Orlow SJ, Boissy RE, Moran DJ, Pifko-Hirst S. Subcellular distribution of tyrosinase and tyrosinase-related protein-1: implications for melanosomal biogenesis. *J Invest Dermatol* 1993;100:55–64. [PubMed: 8423398]
2. Kantheti P, Qiao X, Diaz ME, Peden AA, Meyer GE, Carskadon SL, Kapfhamer D, Sufalko D, Robinson MS, Noebels JL, Burmeister M. Mutation in AP-3 delta in the mocha mouse links endosomal transport to storage deficiency in platelets, melanosomes, and synaptic vesicles. *Neuron* 1998;21:111–122. [PubMed: 9697856]
3. Vijayasaradhi S, Xu Y, Bouchard B, Houghton AN. Intracellular sorting and targeting of melanosomal membrane proteins: identification of signals for sorting of the human brown locus protein, gp75. *J Cell Biol* 1995;130:807–820. [PubMed: 7642699]
4. Jimbow K, Gomez PF, Toyofuku K, Chang D, Miura S, Tsujiya H, Park JS. Biological role of tyrosinase related protein and its biosynthesis and transport from TGN to stage I melanosome, late endosome, through gene transfection study. *Pigment Cell Res* 1997;10:206–213. [PubMed: 9263327]
5. Honing S, Sandoval IV, von Figura K. A di-leucine-based motif in the cytoplasmic tail of LIMP-II and tyrosinase mediates selective binding of AP-3. *EMBO J* 1998;17:1304–1314. [PubMed: 9482728]

6. Jimbow K, Hua C, Gomez PF, Hirosaki K, Shinoda K, Salopek TG, Matsusaka H, Jin HY, Yamashita T. Intracellular vesicular trafficking of tyrosinase gene family protein in eu- and pheomelanosome biogenesis. *Pigment Cell Res* 2000;13:110–117. [PubMed: 11041367]
7. Raposo G, Tenza D, Murphy DM, Berson JF, Marks MS. Distinct protein sorting and localization to premelanosomes, melanosomes, and lysosomes in pigmented melanocytic cells. *J Cell Biol* 2001;152:809– 824. [PubMed: 11266471]
8. Silvers WK. *The Coat Colors of Mice*. New York: Springer-Verlag; 1979.
9. Russell ES. A quantitative histological study of the pigment found in the coat-color mutants of the house mouse. IV. The nature of the effects of genetic substitution in five major allelic series. *Genetics* 1949;34:146–166.
10. Hearing VJ, Phillips P, Lutzner MA. The fine structure of melanogenesis in coat color mutants of the mouse. *J Ultrastruct Res* 1973;43:88–106. [PubMed: 4634048]
11. Lane PW, Womack JE. Ashen, a new color mutation on chromosome 9 of the mouse. *J Hered* 1979;70:133–135.
12. Mercer JA, Seperack PK, Strobel MC, Copeland NG, Jenkins NA. Novel myosin heavy chain encoded by murine *dilute* coat color locus. *Nature* 1991;349:709–713. [PubMed: 1996138]
13. Wilson SM, Yip R, Swing DA, O'Sullivan TN, Zhang Y, Novak EK, Swank RT, Russell LB, Copeland NG, Jenkins NA. A mutation in *Rab27a* causes the vesicle transport defects observed in ashen mice. *Proc Natl Acad Sci USA* 2000;97:7933–7938. [PubMed: 10859366]
14. Matesic LE, Yip R, Reuss AE, Swing DA, O'Sullivan TN, Fletcher CF, Copeland NG, Jenkins NA. Mutations in *Mlph*, encoding a member of the Rab effector family, cause the melanosome transport defects observed in leaden mice. *Proc Natl Acad Sci USA* 2001;98:10238– 10243. [PubMed: 11504925]
15. De La Cruz EM, Wells AL, Rosenfeld SS, Ostap EM, Sweeney HL. The kinetic mechanism of myosin V. *Proc Natl Acad Sci USA* 1999;96:13726–13731. [PubMed: 10570140]
16. Mehta AD, Rock RS, Rief M, Spudich JA, Mooseker MS, Cheney RE. Myosin V is a processive actin-based motor. *Nature* 1999;400:590– 593. [PubMed: 10448864]
17. Sakamoto T, Amitani I, Yokota E, Ando T. Direct observation of processive movement by individual myosin V molecules. *Biochem Biophys Res Commun* 2000;272:586–590. [PubMed: 10833456]
18. Pastural E, Barrat FJ, Dufourcq-Lagelouse R, Certain S, Sanal O, Jabado N, Seger R, Griscelli C, Fischer A, de Saint Basile G. Griscelli disease maps to chromosome 15q21 and is associated with mutations in the Myosin-Va gene. *Nat Genet* 1997;16:289–292. [PubMed: 9207796]
19. Rodman JS, Wandinger-Ness A. Rab GTPases coordinate endocytosis. *J Cell Sci* 2000;113:183–192. [PubMed: 10633070]
20. Chavrier P, Goud B. The role of ARF and rab GTPases in membrane transport. *Curr Opin Cell Biol* 1999;11:466–475. [PubMed: 10449335]
21. Menasche G, Pastural E, Feldmann J, Certain S, Ersoy F, Dupuis S, Wulffraat N, Bianchi D, Fischer A, Le Deist F, de Saint Basile G. Mutations in *RAB27A* cause Griscelli syndrome associated with haemophagocytic syndrome. *Nat Genet* 2000;25:173–176. [PubMed: 10835631]
22. Bahadoran P, Aberdam E, Mantoux F, Busca R, Bille K, Yalman N, de Saint-Basile G, Casaroli-Marano R, Ortonne JP, Ballotti R. *Rab27a*: a key to melanosome transport in human melanocytes. *J Cell Biol* 2001;152:843–850. [PubMed: 11266474]
23. Koyama Y, Takeuchi T. Ultrastructural observations on melanosome aggregation in genetically defective melanocytes of the mouse. *Anat Rec* 1981;4:599–611. [PubMed: 7340565]
24. Provance DW, Wei M, Ipe V, Mercer JA. Cultured melanocytes from *dilute* mutant mice exhibit dendritic morphology and altered melanosome distribution. *Proc Natl Acad Sci USA* 1996;93:14554– 14558. [PubMed: 8962090]
25. Moore KJ, Swing DA, Rinchik EM, Mucenski ML, Buchberg AM, Copeland NG, Jenkins NA. The murine *dilute* suppressor gene *dsu* suppresses the coat-color phenotype of three pigment mutations that alter melanocyte morphology, *d*, *ash* and *ln*. *Genetics* 1988;119:933– 941. [PubMed: 3410303]
26. Huang J, Brady S, Richards B, Stenoien D, Resau J, Copeland N, Jenkins N. Direct interaction of microtubule- and actin-based transport motors. *Nature* 1998;397:267–270. [PubMed: 9930703]

27. Hume AN, Collinson LM, Rapak A, Gomes AQ, Hopkins CR, Seabra MC. Rab27a regulates the peripheral distribution of melanosomes in melanocytes. *J Cell Biol* 2001;152:795–808. [PubMed: 11266470]
28. Wu X, Rao K, Bowers MB, Copeland NG, Jenkins NA, Hammer JA. Rab27a enables myosin Va-dependent melanosome capture by recruiting the myosin to the organelle. *J Cell Sci* 2001;114:1091–1100. [PubMed: 11228153]
29. Walikonis RS, Jensen ON, Mann M, Provance DW Jr, Mercer JA, Kennedy MB. Identification of proteins in the postsynaptic density fraction by mass spectrometry. *J Neurosci* 2000;20:4069–4080. [PubMed: 10818142]
30. Lerner A, Fitzpatrick T. Biochemistry of melanin formation. *Physiol Rev* 1950;30:91–125. [PubMed: 15403662]
31. Dryja TP, O'Neil-Dryja M, Pawelek JM, Albert DM. Demonstration of tyrosinase in the adult bovine uveal tract and retinal pigment epithelium. *Invest Ophthalmol Vis Sci* 1978;17:511–514. [PubMed: 96039]
32. Morrison ME, Yagi MJ, Cohen G. *In vitro* studies of 2,4-dihydroxy-phenylalanine, a prodrug targeted against malignant melanoma cells. *Proc Natl Acad Sci USA* 1985;82:2960–2964. [PubMed: 3921968]
33. Klaus SN. Pigment transfer in mammalian epidermis. *Arch Dermatol* 1969;100:756–762. [PubMed: 5365223]
34. Okazaki K, Uzuka M, Morikawa F, Toda K, Seiji M. Transfer mechanism of melanosomes in epidermal cell culture. *J Invest Dermatol* 1976;67:541–547. [PubMed: 787440]
35. Markert CL, Silvers WK. The effects of genotype and cell environment on melanoblast differentiation in the house mouse. *Genetics* 1956;41:429–450. [PubMed: 17247639]
36. Hollyfield JG, Ward A. Phagocytic activity of the pigmented retinal epithelium. III. Interaction between lysosomes and ingested poly-styrene spheres. *Invest Ophthalmol* 1974;13:1016–1023. [PubMed: 4547761]
37. Novikoff AB, Neuenberger PM, Novikoff PM, Quintana N. Retinal pigment epithelium. Interrelations of endoplasmic reticulum and melanolysosomes in the black mouse and its beige mutant. *Lab Invest* 1979;40:155–165. [PubMed: 107366]
38. Orlow SJ. Melanosomes are specialized members of the lysosomal lineage of organelles. *J Invest Dermatol* 1995;105:3–7. [PubMed: 7615972]
39. Schraermeyer U. Transport of endocytosed material into melanin granules in cultured choroidal melanocytes of cattle – new insights into the relationship of melanosomes with lysosomes. *Pigment Cell Res* 1995;8:209–214. [PubMed: 8610072]
40. Fukuda M, Saegusa C, Mikoshiba K. Novel splicing isoforms of synaptotagmin-like proteins 2 and 3: identification of the Slp homology domain. *Biochem Biophys Res Commun* 2001;283:513–519. [PubMed: 11327731]
41. Wang J, Takeuchi T, Yokota H, Izumi T. Novel rabphilin-3-like protein associates with insulin-containing granules in pancreatic beta cells. *J Biol Chem* 1999;274:28542–28548. [PubMed: 10497219]
42. Shirataki H, Kaibuchi K, Sakoda T, Kishida S, Yamaguchi T, Wada K, Miyazaki M, Takai Y. Rabphilin-3A, a putative target protein for smg p25A/rab3A p25 small GTP-binding protein related to synaptotagmin. *Mol Cell Biol* 1993;13:2061–2068. [PubMed: 8384302]
43. Jimenez M, Tsukamoto K, Hearing VJ. Tyrosinases from two different loci are expressed by normal and by transformed melanocytes. *J Biol Chem* 1991;266:1147–1156. [PubMed: 1898730]

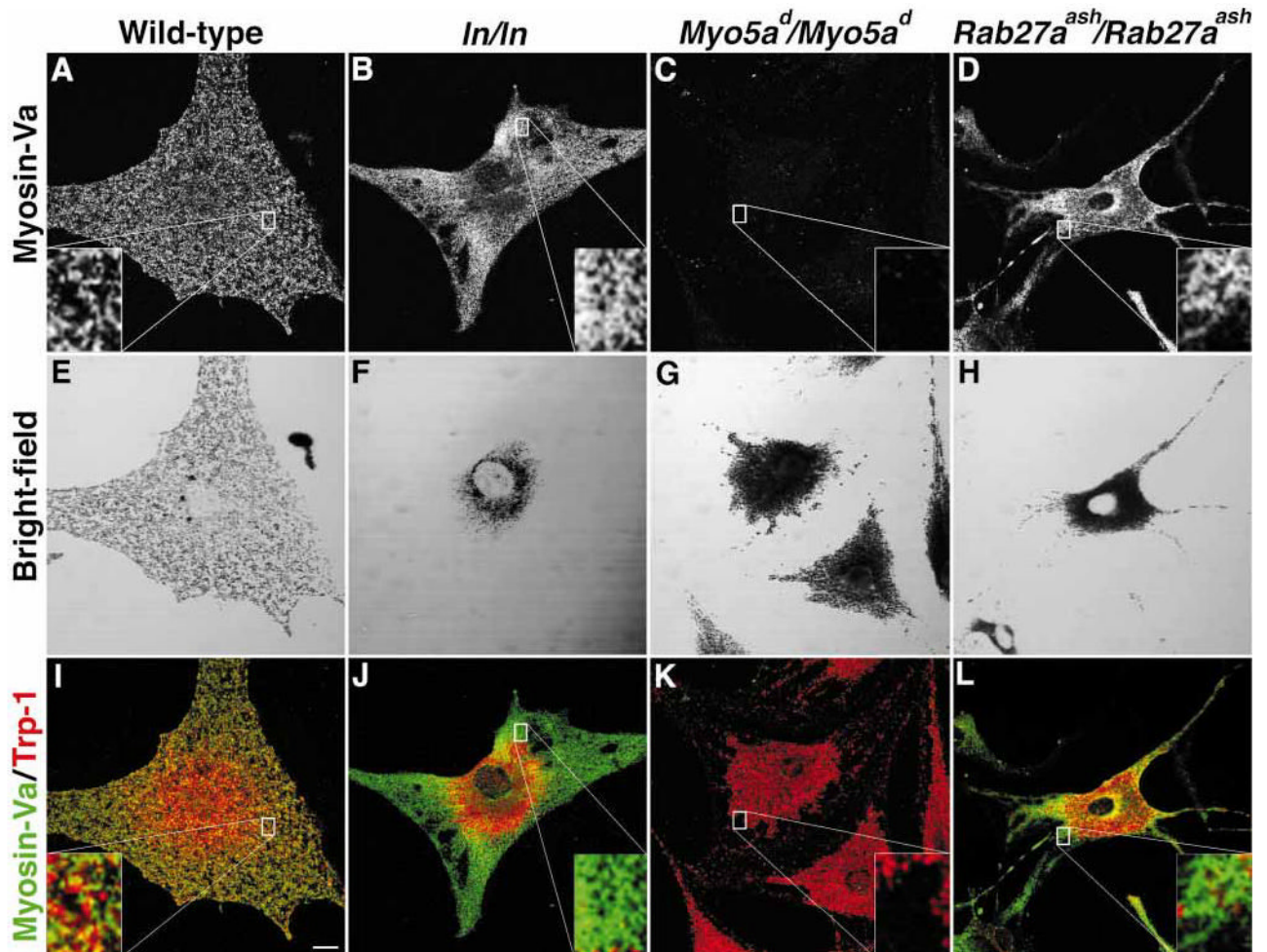


Figure 1. The distribution of myosin-Va is altered in *leaden* and *Rab27a^{ash}/Rab27a^{ash}* primary melanocytes

Indirect immunofluorescent localization of myosin-Va in (A) wild-type (B) *leaden* (C) *Myo5a^d/Myo5a^d*, and (D) *Rab27a^{ash}/Rab27a^{ash}* primary melanocytes. (E–H) Bright-field images showing mature, pigmented melanosomes of cells in panels A, B, C, and D. (I–L) Merged image between myosin-Va (green) and TRP-1 (red), a melanosomal marker. Scale bar, 10 μ m.

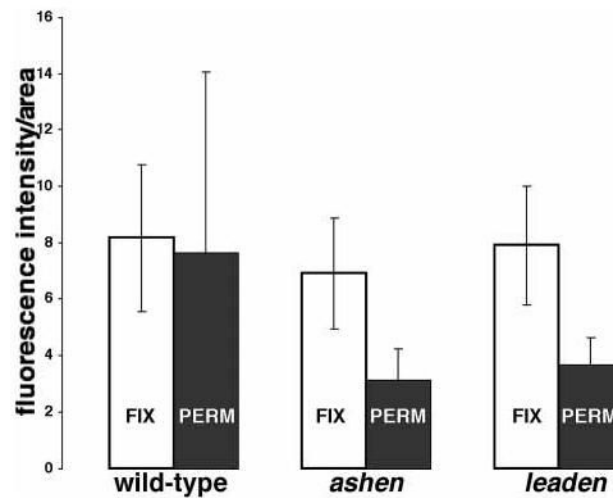


Figure 2. Most myosin-Va immunoreactivity in *leaden* and *Rab27a^{ash}/Rab27a^{ash}* primary melanocytes is lost upon permeabilization of live cells

Indirect immunofluorescent localization of myosin-Va was performed in wild-type control, *ashen* (*Ra-b27a^{ash}/Rab27a^{ash}*) mutant, and *leaden* mutant primary melanocytes, with fixation performed before permeabilization (control, white bars) and permeabilization performed before fixation (black bars). Fluorescence was measured in arbitrary units using LaserSharp software (Bio-Rad). Bars indicate standard deviations. Fluorescence in 15 cells was measured in each condition.

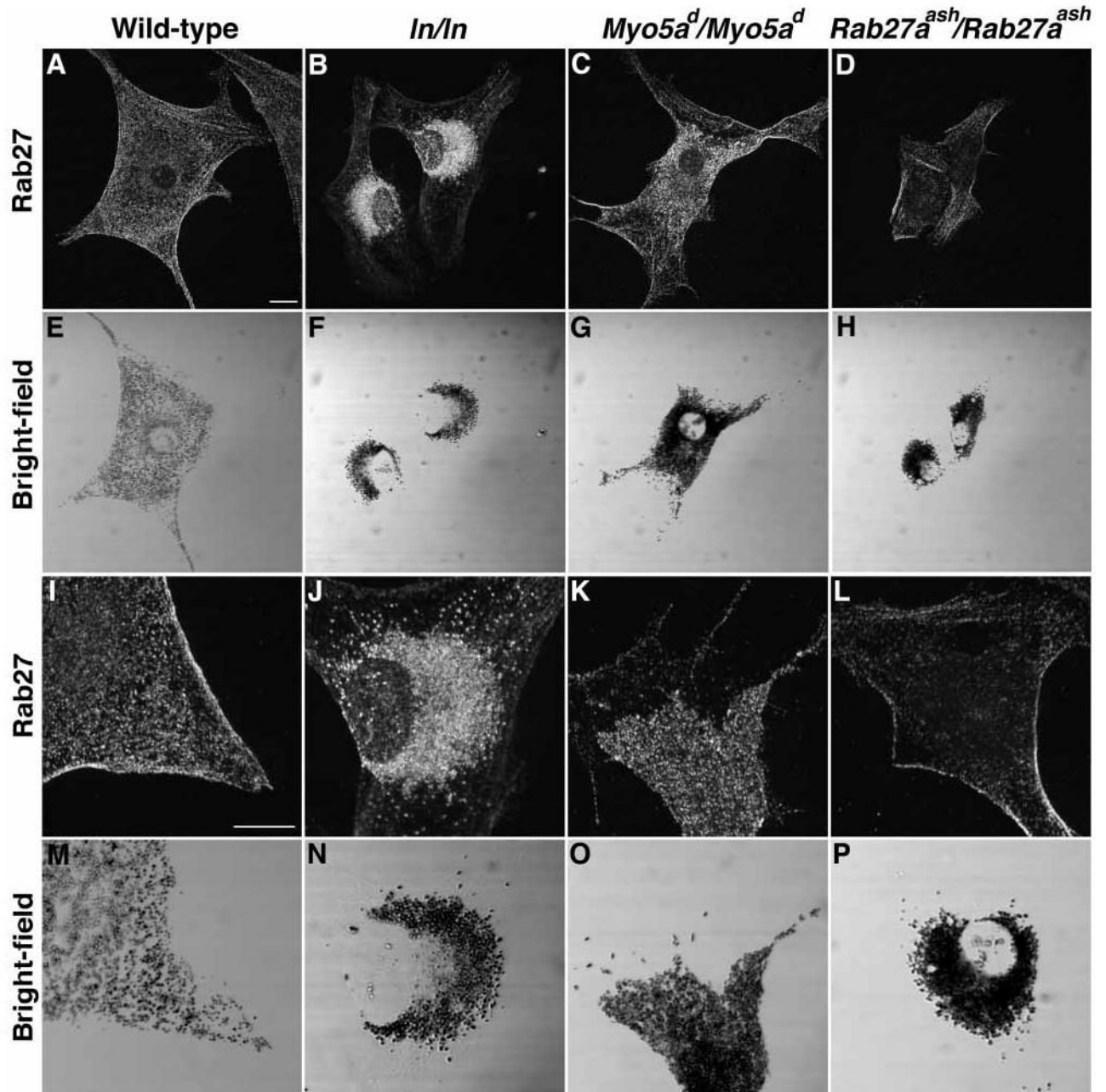


Figure 3. The distribution of rab27a relative to melanosomes is not altered in mutant melanocytes
 Indirect immunofluorescence for rab27a from a single optical section in (A,I) wild-type (B,J) *leaden* (C,K) *Myo5a^d/Myo5a^d*, and (D,L) *Rab27a^{ash}/Rab27a^{ash}* primary melanocytes. (E–H, M–P) Bright-field images showing mature, pigmented melanosomes of cells in panels A–D and I–L. Scale bar, 10 μ m.

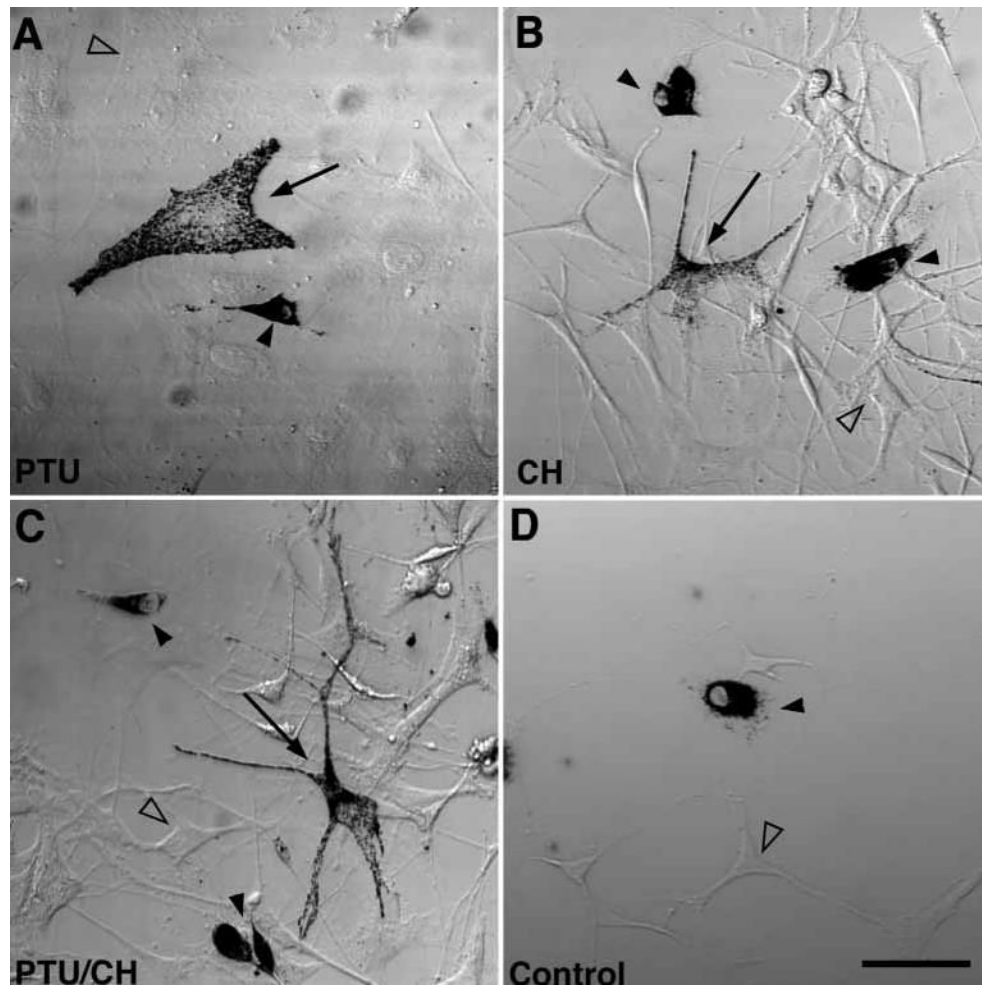


Figure 4. The introduction of melanophilin to *leaden* melanocytes by PEG-mediated cell fusion rescues the perinuclear accumulation of melanosomes

Bright-field images of melan-c cells fused to *leaden* melanocytes with polyethylene glycol and treated for 24 h with (A) PTU to inhibit tyrosinase activity (B) cycloheximide to inhibit protein synthesis, or (C) both. Arrows point to fusion events between melan-c cells and *leaden* melanocytes, filled arrowheads denote *leaden* melanocytes, and open arrowheads point to melan-c cells. (D) Control experiment without fusion, treated with PTU and cycloheximide. Scale bar, 50 μm . CH, cycloheximide.

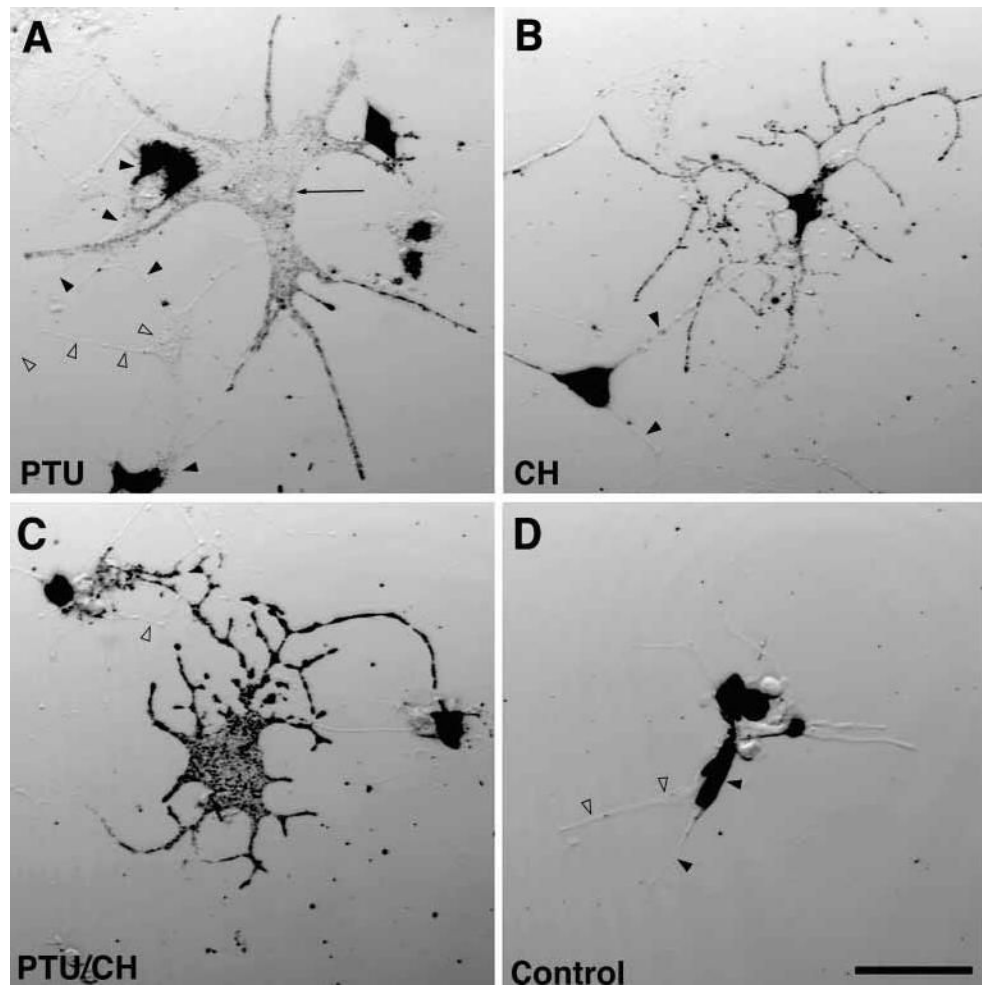


Figure 5. The introduction of rab27a to *Rab27a^{ash}/Rab27a^{ash}* melanocytes by PEG-mediated cell fusion rescues the *ashen* melanocyte phenotype
 Bright-field images of melan-c cells fused to *Rab27a^{ash}/Rab27a^{ash}* melanocytes with polyethylene glycol and treated for 24 h with (A) PTU to inhibit tyrosinase activity (B) cycloheximide to inhibit protein synthesis, or (C) both. Arrows point to fusion events between melan-c cells and *Rab27a^{ash}/Rab27a^{ash}* melanocytes, filled arrowheads denote *Rab27a^{ash}/Rab27a^{ash}* melanocytes, and open arrowheads point to melan-c cells. (D) Control experiment without fusion, treated with PTU and cycloheximide. Scale bar, 50 μ m. CH, cycloheximide.

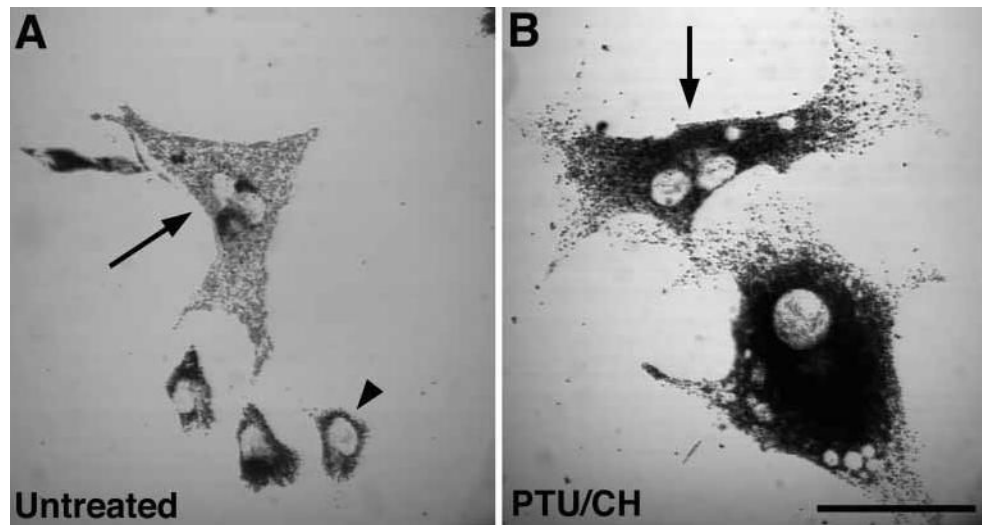


Figure 6. Restoration of melanosome distribution in fusions between *Rab27a^{ash}/Rab27a^{ash}* and *leaden* mutant melanocytes

Bright-field images of leaden melanocytes fused to *Rab27a^{ash}/Rab27a^{ash}* melanocytes with polyethylene glycol (A) untreated and (B) treated for 24 h with both PTU to inhibit tyrosinase activity and cycloheximide to inhibit protein synthesis. Arrows denote heterotypic fusion events and filled arrowheads denote cells with the *leaden* or *ashen* phenotype, which presumably represent unfused cells or homotypic fusion events. Scale bar, 50 μ m. CH, cycloheximide.